

Analysis of the local and parallel space-time algorithm for the heat equation



Dandan Xue^a, Yanren Hou^{a,*}, Yi Li^b

^a School of Mathematics and Statistics, Xi'an Jiaotong University, Xi'an, Shaanxi 710049, China

^b School of Mathematics, Northwest University, Xi'an, Shaanxi 710127, China

ARTICLE INFO

Keywords:

Time-dependent
Parareal
Spectral deferred correction
Local and parallel algorithm
Superposition principle

ABSTRACT

In this paper, a second-order local and parallel space-time algorithm is proposed and analyzed for the heat equation. This scheme is based on the parareal with spectral deferred correction method in time and the expandable local and parallel finite element method in space. It realizes the parallelism both in the temporal as well as in the spatial direction. We prove its stability and the optimal error estimation in L^2 -norm. At last, several numerical experiments are presented to demonstrate the effectiveness of our parallel scheme.

1. Introduction

With the rapid development of high performance computers, parallel algorithms have attracted more attention. It is necessary to exploit parallel algorithm which can use large numbers of cores simultaneously. Although there are many parallel algorithms based on domain decomposition to solve the time dependent partial differential equations, the spatial parallel speedup will saturate as more processors are available. In fact, there is another direction to improve the efficiency, which is parallel in the temporal direction.

In 2001, Lions et al. [1] first provided the parareal algorithm, which is a time integration scheme to compute the numerical solutions of ordinary differential equations or discretized partial differential equations in parallel in the temporal direction. The main idea of parareal method is to decompose the global problem in the time direction into a series of independent subproblems, which can be solved concurrently in each time subinterval. Since this algorithm was proposed, it has received a lot of attention. Convergence and stability of the parareal algorithm have been discussed in [2–6]. The detailed analysis of the scheduling of tasks in parareal algorithm was proposed in [7]. In addition, several variants for parareal method have been proposed, see [8–12]. The parareal algorithm has been successfully applied to a variety of problems, such as quantum system [13], the first and second hyperbolic system [14], Navier-Stokes equations [15], Stokes/Darcy equations [16], the linear structural dynamic system [17], parabolic optimal control problems [18] and so on.

To realize the combination of spatial parallelism with time parallelism, we utilize the expandable local and parallel finite element method for the spatial parallelism. This idea is inspired by the expandable local and parallel two-grid finite element scheme in [19]. In fact, the local and parallel finite element algorithms based on two-grid discretizations was first proposed in [20,21] and further analyzed for other problems, such as the Stokes problem [22,23], the Navier-Stokes problem [24], the eigenvalue problems [25], the time-dependent convection-diffusion equations [26] and so on. The authors of [19] proposed an improved scheme, an expandable local and parallel two-grid finite element scheme for Poisson equations, which can be easily implemented on large parallel computers. What's the difference in this paper is that we use the idea of expandable local and parallel finite element method with the same grid size to realize the spatial parallelism.

The outline of this paper is as follows. Section 2 provides some preliminary materials. In Section 3, we provide the parareal method based on the spectral deferred correction method. Then combining the expandable local and parallel finite element method to realize the spatial parallelism, so we construct the local and parallel space-time algorithm with second order accuracy in time. The stability and convergence results for the space-time parallel algorithm are obtained in Section 4 and 5, respectively. Then the numerical experiments in Section 6 are devoted to support the results of our theoretical analysis. Finally, a brief conclusion and outlook are given in the last section.

* Corresponding author.

E-mail addresses: dandanxue@stu.xjtu.edu.cn (D. Xue), yrhou@mail.xjtu.edu.cn (Y. Hou), liyizz@nwu.edu.cn (Y. Li).

<https://doi.org/10.1016/j.camwa.2021.09.008>

Received 19 June 2020; Received in revised form 14 September 2021; Accepted 17 September 2021

2. Preliminaries

Let $T > 0$ be a finite time, then we consider the initial-boundary value problem for the heat equation with Dirichlet boundary condition in a bounded domain $\Omega \in \mathbb{R}^d$, $d = 2$ or 3 :

$$\begin{cases} u_t - \Delta u = f & \text{in } \Omega \times (0, T], \\ u = 0 & \text{on } \partial\Omega \times (0, T], \\ u(x, 0) = u^0(x) = 0 & \text{in } \Omega, \end{cases} \tag{1}$$

where $u = u(x, t)$ is the temperature and $f = f(x, t)$ is the density of the heat source.

Throughout this paper, for the bounded domain Ω , we denote (\cdot, \cdot) as the usual inner product and $\|\cdot\|_\Omega$ as the corresponding norm in $L^2(\Omega)$. The norm in $H^k(\Omega)$ is denoted by $\|\cdot\|_{k,\Omega}$. The space $H_0^1(\Omega) = \{v \in H^1(\Omega) : v|_{\partial\Omega} = 0\}$ is equipped with the norm $\|\nabla \cdot\|_\Omega$, which is an equivalent norm of $\|\cdot\|_{1,\Omega}$ due to the Poincaré inequality.

The weak formulation of (1) reads: find $u \in H_0^1(\Omega)$ such that

$$\begin{cases} (u_t, v) + a(u, v) = (f, v) \quad \forall v \in H_0^1(\Omega), \\ u(0) = u^0 = 0. \end{cases} \tag{2}$$

Here $a(u, v) = (\nabla u, \nabla v)$.

Let $T^h(\Omega) = \{\tau_\Omega^h\}$ be a regular triangulation of Ω , where $h = \max_{\tau_\Omega^h \in T^h(\Omega)} \{\text{diam}(\tau_\Omega^h)\}$ is the mesh size parameter. Associated with the mesh $T^h(\Omega)$, we set

$$\begin{aligned} S^h(\Omega) &= \{v_h \in C^0(\Omega) : v_h|_{\tau_\Omega^h} \in P_{\tau_\Omega^h}^r, \forall \tau_\Omega^h \in T^h(\Omega)\}, \\ S_0^h(\Omega) &= S^h(\Omega) \cap H_0^1(\Omega). \end{aligned}$$

Here, $r \geq 1$ is a positive integer and $P_{\tau_\Omega^h}^r$ is the space of polynomial of degree not greater than r defined on τ_Ω^h .

We introduce the Ritz projection P_h from $H_0^1(\Omega)$ onto $S_0^h(\Omega)$ by requiring

$$a(u, P_h v - v) = 0, \quad \forall u \in S_0^h(\Omega), v \in H_0^1(\Omega). \tag{3}$$

The Ritz projection is stable in $H_0^1(\Omega)$, that is to say

$$\|\nabla P_h v\|_\Omega \leq \|\nabla v\|_\Omega, \quad \forall v \in H_0^1(\Omega).$$

In addition, the Ritz projection has the property:

$$\|P_h v - v\|_\Omega + h \|\nabla(P_h v - v)\|_\Omega \leq C_R h^{r+1} \|v\|_{r+1,\Omega}, \quad \forall v \in H_0^1(\Omega) \cap H^{r+1}(\Omega). \tag{4}$$

We recall the Poincaré inequality: there exists constant C_p , which only depends on the region Ω , such that

$$\|v\|_\Omega \leq C_p \|\nabla v\|_\Omega, \quad \forall v \in H_0^1(\Omega), \tag{5}$$

the Young's inequality with ε :

$$ab \leq \varepsilon a^2 + \frac{1}{4\varepsilon} b^2, \quad (a, b > 0, \varepsilon > 0), \tag{6}$$

and the Minkowski inequality: assume $1 \leq p \leq \infty$ and $u, v \in L^p(\Omega)$, then

$$\|u + v\|_{L^p(\Omega)} \leq \|u\|_{L^p(\Omega)} + \|v\|_{L^p(\Omega)}. \tag{7}$$

3. The local and parallel space-time scheme

In this section, we propose a space-time parallel algorithm for the heat equation with second order accuracy in time. And we denote it as the local and parallel space-time scheme. The temporal parallelism is achieved with the parareal method, the spatial parallelism is achieved with the expandable local and parallel method, and the spectral deferred correction method is used to get the second-order scheme. However, in order to introduce the final space-time parallel algorithm more clearly, we first introduce the parareal method. Then combining the idea of the expandable local and parallel finite element method, we provide the special steps of the space-time parallel algorithm.

3.1. The parareal method

Let $\Delta t = T/N$ be the time step length, and we divide the time interval $[0, T]$ into N subintervals $[t^n, t^{n+1}]$ by choosing points $t^n = n\Delta t$ for $n = 0, \dots, N - 1$. For the parareal method, the subintervals are assigned to different processors. For simplicity, denote the processors P_1 through P_N . Generally, we need two numerical ordinary differential equation step methods denoted by \mathcal{G} and \mathcal{F} . In addition, for the sake of efficiency of the parareal method, \mathcal{G} is computationally less expensive than \mathcal{F} . In order to reduce the computational cost of \mathcal{G} , one can choose \mathcal{G} with a larger time step length or a coarser discretization in space or even a lower-order numerical method than \mathcal{F} . Upon convergence, the accuracy of the parareal method is limited by what one would obtain if \mathcal{F} is used in serial. We are going to use the notations $\mathcal{G}(t^{n+1}, t^n, \hat{u})$ and $\mathcal{F}(t^{n+1}, t^n, \hat{u})$, which means the numerical solutions at time t^{n+1} with the initial value \hat{u} at time t^n by using \mathcal{G} and \mathcal{F} , respectively.

For the first step of parareal method, \mathcal{G} is used to compute a provisional solution of (1) at all nodes sequentially, i.e.,

$$u_1^{n+1} = \mathcal{G}(t^{n+1}, t^n, u_1^n), \quad n = 0, \dots, N - 1.$$

As soon as each processor P_{n+1} obtains the initial value u_k^n and the provisional solution u_k^{n+1} with the iteration number $k \geq 1$, one can compute a more accurate approximate solution $\mathcal{F}(t^{n+1}, t^n, u_k^n)$ at each t^{n+1} in parallel. Then the final serial correction step takes the form

$$u_{k+1}^{n+1} = \mathcal{G}(t^{n+1}, t^n, u_{k+1}^n) + \mathcal{F}(t^{n+1}, t^n, u_k^n) - \mathcal{G}(t^{n+1}, t^n, u_k^n), \tag{8}$$

for $n = 0, \dots, N - 1$. The parareal method proceeds iteratively alternating between the parallel computation of $\mathcal{F}(t^{n+1}, t^n, u_k^n)$ and the serial computation of (8), requires computing the \mathcal{G} propagator.

Next, we provide a second-order time parallel algorithm based on parareal method for the heat equation (1). First, we select the backward Euler method as \mathcal{G} . Note again that, upon convergence, the accuracy of parareal method is limited by what one would obtain if \mathcal{F} is used in serial. We utilize the second-order spectral deferred correction (SDC) sweep as \mathcal{F} . Therefore we provide a simple introduction of SDC method.

The SDC method [27–29] is one kind of high-order numerical methods, which uses a low order numerical method to get an approximation solution with higher-order accuracy by solving a series of deferred correction equations during each time step. Next we introduce the classical formulation of SDC method by quoting symbols from the literature [29]. The initial value problem reads

$$\begin{cases} \phi'(t) = F(t, \phi(t)), & t \in [0, T], \\ \phi(0) = \phi^0, \end{cases}$$

with $\phi(t), \phi^0 \in \mathbb{C}^d$ and $F : \mathbb{R} \times \mathbb{C}^d \rightarrow \mathbb{C}^d$. Let us first divide the time interval $[0, T]$ into several intervals $[t^n, t^{n+1}] = [t^n, t^n + \Delta t]$ with $\Delta t = T/N$. Then choosing points t^m for $m = 0, \dots, p$ with $t^n = t^0 < t^1 < \dots < t^p = t^{n+1}$, so we obtain p subintervals $[t^m, t^{m+1}] = [t^m, t^m + \Delta t^m]$. If the approximate solutions $\phi_1^m, m = 0, \dots, p$, have been obtained by using the backward Euler method, then the SDC method based on the Euler methods is the following formulation:

$$\phi_{k+1}^{m+1} = \phi_{k+1}^m + \Delta t^m [F(t^{m+1}, \phi_{k+1}^{m+1}) - F(t^{m+1}, \phi_k^{m+1})] + I_m^{m+1}(\phi_k). \tag{9}$$

$I_m^{m+1}(\phi_k)$ denotes the numerical quadrature approximation to $\int_{t^m}^{t^{m+1}} F(\tau, \phi_k(\tau))d\tau$, and ϕ_k denotes the approximation solution with k total iterations or $k - 1$ iterations of correction equation. As long as the accuracy of quadrature approximation $I_m^{m+1}(\phi_k)$ can be guaranteed, ϕ_{k+1}^{m+1} is a numerical solution with the global accuracy $O(\Delta t^{k+1})$. The readers are referred to [27–29] for the detailed discussion of order of accuracy for SDC method. In this paper, in order to construct a second-order scheme based on SDC, there is no need to divide interval $[t^n, t^{n+1}]$ into subintervals and we only use the two integral points t^n and t^{n+1} to approximate $\int_{t^n}^{t^{n+1}} F(\tau, \phi_k(\tau))d\tau$ by utilizing the trapezoid formula, that is

$$I_n^{n+1}(\phi_k) = \frac{1}{2} \Delta t [F(t^{n+1}, \phi_k(t^{n+1})) + F(t^n, \phi_k(t^n))]. \tag{10}$$

In addition, if ϕ_1^n and ϕ_1^{n+1} for $n = 1, 2, \dots, N - 1$ have been obtained by using the backward Euler method, one iteration step (9) is sufficient to obtain ϕ_2^{n+1} with the accuracy $O(\Delta t^2)$. Hence, combining (9)-(10) leads to a second-order SDC sweep as follows:

$$\phi_2^{n+1} = \phi_2^n + \Delta t F(t^{n+1}, \phi_2^{n+1}) - \frac{1}{2} \Delta t F(t^{n+1}, \phi_1^{n+1}) + \frac{1}{2} \Delta t F(t^n, \phi_1^n). \tag{11}$$

Now we are ready to propose the second-order parareal algorithm for the heat equation. Let us select the backward Euler method as \mathcal{G} and a second-order SDC sweep as \mathcal{F} . For the time interval $[0, T]$, we divide it into N subintervals $[t^n, t^{n+1}] = [t^n, t^n + \Delta t], n = 0, 1, \dots, N - 1$ with the time step length $\Delta t = T/N$. For the first step of the parareal method, let us serially compute the provisional solutions $u_{1,h}^{n+1} := \mathcal{G}(t^{n+1}, t^n, u_{1,h}^n) \in S_0^h(\Omega), n = 0, \dots, N - 1$, by using the backward Euler method as follows: find $u_{1,h}^{n+1} \in S_0^h(\Omega)$ such that $\forall v_h \in S_0^h(\Omega)$

$$\begin{cases} (\frac{u_{1,h}^{n+1} - u_{1,h}^n}{\Delta t}, v_h) + a(u_{1,h}^{n+1}, v_h) = (f^{n+1}, v_h), \\ u_{1,h}^0 = P_h u^0 = 0. \end{cases} \tag{12}$$

Then, we consider a second-order SDC sweep (11) as \mathcal{F} to compute $\mathcal{F}(t^{n+1}, t^n, u_{1,h}^n), n = 0, 1, \dots, N - 1$ in parallel. It is important to emphasize that we compute \mathcal{F} with the initial values $u_{1,h}^n$, which has been obtained by the first step. So that we can simultaneously compute $\mathcal{F}(t^{n+1}, t^n, u_{1,h}^n)$ on the N subintervals $[t^n, t^{n+1}]$. Hence, for the heat equation, $\tilde{u}_F^{n+1} := \mathcal{F}(t^{n+1}, t^n, u_{1,h}^n) \in S_0^h(\Omega)$ satisfies

$$\tilde{u}_F^{n+1} = u_{1,h}^n + \Delta t F(t^{n+1}, \tilde{u}_F^{n+1}) - \frac{1}{2} \Delta t F(t^{n+1}, u_{1,h}^{n+1}) + \frac{1}{2} \Delta t F(t^n, u_{1,h}^n),$$

where $F(t, u(x, t)) = f(x, t) + \Delta u(x, t)$. It is easy to obtain the following weak formulation: find $\tilde{u}_F^{n+1} \in S_0^h(\Omega)$ over $\Omega \times [t^n, t^{n+1}]$ such that $\forall v_h \in S_0^h(\Omega)$

$$(\frac{\tilde{u}_F^{n+1} - u_{1,h}^n}{\Delta t}, v_h) + a(\tilde{u}_F^{n+1}, v_h) = a(\frac{u_{1,h}^{n+1} - u_{1,h}^n}{2}, v_h) + (\frac{f^{n+1} + f^n}{2}, v_h). \tag{13}$$

Last, considering the third step of parareal method (8), we compute the final solution as follows:

$$\tilde{u}_{2,h}^{n+1} = \mathcal{G}(t^{n+1}, t^n, \tilde{u}_{2,h}^n) + \mathcal{F}(t^{n+1}, t^n, u_{1,h}^n) - \mathcal{G}(t^{n+1}, t^n, u_{1,h}^n) \in S_0^h(\Omega), \quad n = 0, \dots, N - 1. \tag{14}$$

Remark 3.1. In principle, the parareal method proceeds iteratively alternating between the parallel computation of \mathcal{F} and the serial computation of (14), which requires computing \mathcal{G} . Note that the accuracy of \mathcal{F} determines the overall accuracy. The convergence order of the parareal method [3,5] is decided by the order of \mathcal{G} and the number of iterations used when it is coupled with a sufficient accuracy \mathcal{F} . And the convergence results are obtained under some assumptions for \mathcal{G} and \mathcal{F} . For example, let \mathcal{F} be the exact solution and let \mathcal{G} satisfy the Lipschitz condition. Since we select the first-order backward Euler method as \mathcal{G} for the heat equation, it is easy to verify that \mathcal{G} satisfies the Lipschitz condition, and the convergence order in time will increase by one time with each iteration. Since we want to construct a second order algorithm, so only 2 iterations are used in our algorithms.

Normally in real calculation, if we want to use the parareal method to obtain almost the same accuracy of \mathcal{F} , it indeed needs more iterations of the alternative steps between \mathcal{F} and \mathcal{G} . However, there are only two iterations in our algorithm, no more iterations. In Section 6, we compute the algorithm with more than two iterations, but the errors are bigger than that one with two iterations. And the algorithm with two iterations is enough to obtain almost the same accuracy of \mathcal{F} , which is used in serial. Therefore, the expected results can be obtained through two iterations while considering the calculation time and the accuracy of our parallel algorithm.

3.2. The local and parallel space-time scheme

In this part, we propose a local and parallel space-time algorithm for the heat equation. For the time parallelism, it is based on parareal method, so we can compute the solutions over all time steps in parallel. Then we combine it with the expandable local and parallel method [19] to realize the spatial parallelism over each subdomain. In our local and parallel space-time scheme, we choose the backward Euler method as \mathcal{G} , and a second-order SDC sweep with the expandable local and parallel method as \mathcal{F} . Let us denote $u_{2,h}^{n+1} \in S_0^h(\Omega)$, $n = 0, \dots, N - 1$ as the ultimate approximate solution of our space-time parallel scheme. The following parts are the specific steps of this algorithm.

For the first step, we compute the global solution $u_{1,h}^{n+1} := \mathcal{G}(t^{n+1}, t^n, u_{1,h}^n) \in S_0^h(\Omega)$, $n = 0, \dots, N - 1$, by using the backward Euler method (12) serially.

The second step is to compute the solutions $u_F^{n+1} := \mathcal{F}(t^{n+1}, t^n, u_{1,h}^n) \in S_0^h(\Omega)$, $n = 0, \dots, N - 1$ in parallel. Since the initial value $u_{1,h}^n$ has been obtained from the first step, we can calculate u_F^{n+1} over N subintervals $[t^n, t^{n+1}]$, $n = 0, \dots, N - 1$, concurrently. Meanwhile, over each time step, we utilize the expandable local and parallel scheme to realize the spatial parallelism. From the idea of this spatial parallel method, we first need to construct a residual equation. Let us denote $w^{n+1} = u_F^{n+1} - u_{1,h}^{n+1} \in S_0^h(\Omega)$, then we can construct a residual equation from (13): $\forall v_h \in S_0^h(\Omega)$,

$$\left(\frac{w^{n+1}}{\Delta t}, v_h\right) + a(w^{n+1}, v_h) = -\left(\frac{u_{1,h}^{n+1} - u_{1,h}^n}{\Delta t}, v_h\right) - a(u_{1,h}^{n+1}, v_h) + a\left(\frac{u_{1,h}^{n+1} - u_{1,h}^n}{2}, v_h\right) + \left(\frac{f^{n+1} + f^n}{2}, v_h\right). \tag{15}$$

In other words, (15) is also a correction step for the provisional solution $u_{1,h}^{n+1}$. Next, we are going to divide this problem (15) into several subproblems on different computational domains to realize the spatial parallelism.

Assume that $\{\phi_j\}_{j=1}^M$ is a partition of unity on Ω for given $M \geq 1$ such that $\Omega \subset \bigcup_{j=1}^M \text{supp}\phi_j$ and $\sum_{j=1}^M \phi_j \equiv 1$ on Ω . What's more, we define a coarser grid triangulation $T^H(\Omega)$, which aligns with the global regular triangulation $T^h(\Omega)$ on Ω with $H > h$. Let us denote $D_j = \text{supp}\phi_j$ which aligns with $T^H(\Omega)$. Then the residual equation (15) can be rewritten as:

$$\left(\frac{w^{n+1}}{\Delta t}, v_h\right) + a(w^{n+1}, v_h) = -\left(\frac{u_{1,h}^{n+1} - u_{1,h}^n}{\Delta t}, \sum_{j=1}^M \phi_j v_h\right) - a(u_{1,h}^{n+1}, \sum_{j=1}^M \phi_j v_h) + a\left(\frac{u_{1,h}^{n+1} - u_{1,h}^n}{2}, \sum_{j=1}^M \phi_j v_h\right) + \left(\frac{f^{n+1} + f^n}{2}, \sum_{j=1}^M \phi_j v_h\right).$$

By superposition principle, the above equation is equivalent to the summation of the following subproblems: $\forall v_h \in S_0^h(\Omega)$, $j = 1, \dots, M$,

$$\left(\frac{w^{j,n+1}}{\Delta t}, v_h\right) + a(w^{j,n+1}, v_h) = -\left(\frac{u_{1,h}^{n+1} - u_{1,h}^n}{\Delta t}, \phi_j v_h\right) - a(u_{1,h}^{n+1}, \phi_j v_h) + a\left(\frac{u_{1,h}^{n+1} - u_{1,h}^n}{2}, \phi_j v_h\right) + \left(\frac{f^{n+1} + f^n}{2}, \phi_j v_h\right). \tag{16}$$

And $w^{n+1} = \sum_{j=1}^M w^{j,n+1}$. Obviously, each subproblem is driven by right-hand side term of a very small compact support with homogeneous Dirichlet boundary condition in the entire domain Ω . In order to reduce the computational scale, we restrict the above subproblem in a local domain $\Omega_j \supset D_j$ instead of the global domain Ω . For each local domain Ω_j , we consider $T^h(\Omega_j) = T^h(\Omega)|_{\Omega_j} = \{\tau_{\Omega_j}^h\}$ and $h = \max_{1 \leq j \leq M} \max_{\tau_{\Omega_j}^h \in T^h(\Omega_j)} \{\text{diam}(\tau_{\Omega_j}^h)\}$. And we define

the following finite element spaces

$$S^h(\Omega_j) = \{v_h \in C^0(\Omega_j) : v_h|_{\tau_{\Omega_j}^h} \in P_{\tau_{\Omega_j}^h}^r, \forall \tau_{\Omega_j}^h \in T^h(\Omega_j)\},$$

$$S_0^h(\Omega_j) = S^h(\Omega_j) \cap H_0^1(\Omega_j).$$

On the other hand, one can extend the functions in $S_0^h(\Omega_j)$ to functions in $S_0^h(\Omega)$ with zero value outside Ω_j . In this sense, we can regard $S_0^h(\Omega_j)$ as a subspace of $S_0^h(\Omega)$. Hence, we can assume

$$S_0^h(\Omega) = \bigcup_{1 \leq j \leq M} S_0^h(\Omega_j).$$

Now we choose the piecewise linear Lagrange basis functions as the partition of unity $\{\phi_j\}_{j=1}^M$ of Ω , and it is associated with the global coarser grid triangulation $T^H(\Omega)$. Here M is the number of vertices of $T^H(\Omega)$ and includes the boundary vertices. Hence, for each vertex j of the coarse grid $T^H(\Omega)$, we still denote $D_j = \text{supp}\phi_j$ and assume the local domain Ω_j is obtained by extending D_j by one mesh layer, i.e.

$$\Omega_j = \bigcup \left\{ D \mid D \text{ and } D_j \text{ share at least one vertex, } D \in \{D_1, D_2, \dots, D_M\} \right\}.$$

It is obvious that

$$\text{diam}D_j \cong H, \quad \text{dist}(\partial D_j \setminus \partial \Omega, \partial \Omega_j \setminus \partial \Omega) \cong H.$$

Here, $x \approx y$ means that $c_1x \leq y \leq C_1x$, for constants c_1 and C_1 that are independent of mesh size and time step length. So let us approximate the local residual equation (16) over $\Omega_j \times [t^n, t^{n+1}]$, $j = 1, \dots, M$, as follows: find $w_h^{j,n+1} \in S_0^h(\Omega_j)$ such that $\forall v_h \in S_0^h(\Omega_j)$

$$\left(\frac{w_h^{j,n+1}}{\Delta t}, v_h\right) + a(w_h^{j,n+1}, v_h) = -\left(\frac{u_{1,h}^{n+1} - u_{1,h}^n}{\Delta t}, \phi_j v_h\right) - a(u_{1,h}^{n+1}, \phi_j v_h) + a\left(\frac{u_{1,h}^{n+1} - u_{1,h}^n}{2}, \phi_j v_h\right) + \left(\frac{f^{n+1} + f^n}{2}, \phi_j v_h\right). \tag{17}$$

Obviously, since $u_{1,h}^{n+1}$ and $u_{1,h}^n$ have been obtained from (12), all subproblems (17) are mutually independent over each computational domain. Therefore, we can solve (17), concurrently, over each sub-domain Ω_j . Next let us extend $w_h^{j,n+1}$ to the entire domain Ω with zero value outside Ω_j in $H_0^1(\Omega)$ and still denote $w_h^{j,n+1}$ as the extension. Then define the approximate solution

$$u_F^{n+1} = w_h^{n+1} + u_{1,h}^{n+1} = \sum_{j=1}^M w_h^{j,n+1} + u_{1,h}^{n+1} \in S_0^h(\Omega).$$

The third step of parareal method, which is also the last step of the space-time parallel algorithm, is to compute $u_G^{n+1} := \mathcal{G}(t^{n+1}, t^n, u_{2,h}^n) \in S_0^h(\Omega)$ by using the backward Euler method such that

$$\left(\frac{u_G^{n+1} - u_{2,h}^n}{\Delta t}, v_h\right) + a(u_G^{n+1}, v_h) = (f^{n+1}, v_h), \quad \forall v_h \in S_0^h(\Omega). \tag{18}$$

Last, we derive the final approximate solution

$$\begin{aligned} u_{2,h}^{n+1} &= \mathcal{G}(t^{n+1}, t^n, u_{2,h}^n) + \mathcal{F}(t^{n+1}, t^n, u_{1,h}^n) - \mathcal{G}(t^{n+1}, t^n, u_{1,h}^n) \\ &:= u_G^{n+1} + u_F^{n+1} - u_{1,h}^{n+1} \in S_0^h(\Omega). \end{aligned} \tag{19}$$

In conclusion, we summarize the specific steps of our local and parallel space-time scheme in Algorithm 3.1.

Algorithm 3.1 (The local and parallel space-time scheme for the heat equation).

- Step 1. Compute $u_{1,h}^{n+1} := \mathcal{G}(t^{n+1}, t^n, u_{1,h}^n) \in S_0^h(\Omega)$, $n = 0, \dots, N - 1$, by using (12) in serial.
- Step 2. Compute $u_F^{n+1} := \mathcal{F}(t^{n+1}, t^n, u_{1,h}^n) \in S_0^h(\Omega)$, $n = 0, \dots, N - 1$ in parallel. Time parallelism is achieved by computing u_F^{n+1} over the N intervals $[t^n, t^{n+1}]$, $n = 0, \dots, N - 1$, concurrently. Let's take the interval $[t^n, t^{n+1}]$ as an example to show how the spatial parallelism is implemented.
 - a) Solve (17) concurrently over $\Omega_j \times [t^n, t^{n+1}]$, $j = 1, \dots, M$ to obtain $w_h^{j,n+1} \in S_0^h(\Omega_j)$.
 - b) We extend $w_h^{j,n+1}$ to the entire domain Ω with zero value outside Ω_j in $H_0^1(\Omega)$, and still use $w_h^{j,n+1}$ to denote the extension. Then we define $u_F^{n+1} = w_h^{n+1} + u_{1,h}^{n+1} = \sum_{j=1}^M w_h^{j,n+1} + u_{1,h}^{n+1} \in S_0^h(\Omega)$.
- Step 3. Compute $u_G^{n+1} := \mathcal{G}(t^{n+1}, t^n, u_{2,h}^n) \in S_0^h(\Omega)$, $n = 0, \dots, N - 1$, by using (18) in serial. Last, we obtain the final approximate solution $u_{2,h}^{n+1} = u_G^{n+1} + u_F^{n+1} - u_{1,h}^{n+1}$ with the initial value $u_{2,h}^0 = P_h u^0 = 0$.

4. The stability analysis

Before we present the analysis for our local and parallel space-time scheme, we give the analysis results of the standard Galerkin approximation (12), which will be used in the next analysis. Since the proof is classic, we omit the details and only show the final results. We refer the readers to [30–32] for the details.

Lemma 4.1. Assume $u_{1,h}^m$, $m = 1, \dots, N$ is the solution of (12), then the following results hold:

a) It satisfies the stability result

$$\|u_{1,h}^m\|_{\Omega}^2 + \Delta t \sum_{n=0}^{m-1} \|\nabla u_{1,h}^{n+1}\|_{\Omega}^2 \leq C \Delta t \sum_{n=0}^m \|f^n\|_{\Omega}^2. \tag{20}$$

b) Assume the exact solution of (2) satisfies the following regularities

$$u \in L^\infty(0, T; H^{r+1}(\Omega)^d), \quad u_t \in L^2(0, T; H^{r+1}(\Omega)^d), \quad u_{tt} \in L^2(0, T; H^r(\Omega)^d), \quad u_{ttt} \in L^2(0, T; L^2(\Omega)^d), \tag{21}$$

and denote $e_{1,h}^m = u_{1,h}^m - u^m$, $d_t e_{1,h}^m = \frac{e_{1,h}^m - e_{1,h}^{m-1}}{\Delta t}$. We have

$$\|e_{1,h}^m\|_{\Omega}^2 \leq C(\Delta t^2 + h^{2r+2}), \quad \|d_t e_{1,h}^m\|_{\Omega}^2 + \Delta t \sum_{n=0}^{m-1} \|\nabla(d_t e_{1,h}^{n+1})\|_{\Omega}^2 \leq C(\Delta t^2 + h^{2r}). \tag{22}$$

In addition, if assume

$$u_{ttt} \in L^2(0, T; L^2(\Omega)^d), \tag{23}$$

and denote $S_{1,h}^m = \frac{d_t e_{1,h}^m - d_t e_{1,h}^{m-1}}{\Delta t}$, we obtain

$$\|S_{1,h}^m\|_{\Omega}^2 + \Delta t \sum_{n=0}^{m-1} \|\nabla(S_{1,h}^{n+1})\|_{\Omega}^2 \leq C(\Delta t^2 + h^{2r}). \tag{24}$$

In order to extend the local residual equation (17) from Ω_j to the entire domain Ω , we will use the fictitious domain method [33,34]. However the extension requires a new variable defined only at the boundary of the sub-domain Ω_j . So we give some symbols and finite element spaces for the boundary. Denote $\Gamma = \partial\Omega$, $\Gamma_j = \partial\Omega_j \setminus \Gamma$, $H_h^{\frac{1}{2}}(\Gamma_j) = S_0^h(\Omega)|_{\Gamma_j} \subset H^{\frac{1}{2}}(\Gamma_j)$ and $H_h^{-\frac{1}{2}}(\Gamma_j)$. Here $H_h^{-\frac{1}{2}}(\Gamma_j)$ is the dual space of $H_h^{\frac{1}{2}}(\Gamma_j)$ and is equipped with the following norm:

$$\|\mu\|_{H_h^{-\frac{1}{2}}(\Gamma_j)} = \sup_{v \in H_h^{\frac{1}{2}}(\Gamma_j)} \frac{\int_{\Gamma_j} \mu v ds}{\|v\|_{H_h^{\frac{1}{2}}(\Gamma_j)}}.$$

We rewrite the local residual equation (17) as: find $w_h^{j,n+1} \in S_0^h(\Omega_j)$ such that $\forall v_h \in S_0^h(\Omega_j)$

$$(w_h^{j,n+1}, v_h) + \Delta t a(w_h^{j,n+1}, v_h) = -\Delta t \left(\frac{u_{1,h}^{n+1} - u_{1,h}^n}{\Delta t}, \phi_j v_h \right) - \Delta t a(u_{1,h}^{n+1}, \phi_j v_h) + \Delta t a\left(\frac{u_{1,h}^{n+1} - u_{1,h}^n}{2}, \phi_j v_h\right) + \Delta t \left(\frac{f^{n+1} + f^n}{2}, \phi_j v_h\right).$$

Using the idea of fictitious domain method, we need to consider the Dirichlet boundary condition on Γ_j in a weak sense instead of being composed in the space $S_0^h(\Omega_j)$. Hence we provide the following saddle point problem: find $(w_h^{j,n+1}, \lambda_h^{j,n+1}) \in S_0^h(\Omega) \times H_h^{-\frac{1}{2}}(\Gamma_j)$ such that $\forall v_h \in S_0^h(\Omega)$, $\mu_h \in H_h^{-\frac{1}{2}}(\Gamma_j)$

$$\begin{cases} (w_h^{j,n+1}, v_h) + \Delta t a(w_h^{j,n+1}, v_h) - \langle \lambda_h^{j,n+1}, v_h \rangle_{\Gamma_j} \\ = -\Delta t \left(\frac{u_{1,h}^{n+1} - u_{1,h}^n}{\Delta t}, \phi_j v_h \right) - \Delta t a(u_{1,h}^{n+1}, \phi_j v_h) + \Delta t a\left(\frac{u_{1,h}^{n+1} - u_{1,h}^n}{2}, \phi_j v_h\right) + \Delta t \left(\frac{f^{n+1} + f^n}{2}, \phi_j v_h\right), \\ \langle \mu_h, w_h^{j,n+1} \rangle_{\Gamma_j} = 0. \end{cases} \tag{25}$$

Here

$$\langle \mu, v \rangle_{\Gamma_j} = \int_{\Gamma_j} \mu v ds, \quad \forall \mu \in H_h^{-\frac{1}{2}}(\Gamma_j), v \in S_0^h(\Omega).$$

Throughout this paper we use the letter C to denote the generic positive constant which is different in different places but remains independent of mesh size and time step length.

If we denote $w^{j,n+1}|_{\Gamma_j} = g^{j,n+1}$, then the equivalent saddle point problem for (16) is: find $(w^{j,n+1}, \zeta_h^{j,n+1}) \in S_0^h(\Omega) \times H_h^{-\frac{1}{2}}(\Gamma_j)$ such that $\forall (v_h, \mu_h) \in S_0^h(\Omega) \times H_h^{-\frac{1}{2}}(\Gamma_j)$

$$\begin{cases} (w^{j,n+1}, v_h) + \Delta t a(w^{j,n+1}, v_h) - \langle \zeta_h^{j,n+1}, v_h \rangle_{\Gamma_j} \\ = -\Delta t \left(\frac{u_{1,h}^{n+1} - u_{1,h}^n}{\Delta t}, \phi_j v_h \right) - \Delta t a(u_{1,h}^{n+1}, \phi_j v_h) + \Delta t a\left(\frac{u_{1,h}^{n+1} - u_{1,h}^n}{2}, \phi_j v_h\right) + \Delta t \left(\frac{f^{n+1} + f^n}{2}, \phi_j v_h\right), \\ \langle \mu_h, w^{j,n+1} - g^{j,n+1} \rangle_{\Gamma_j} = 0. \end{cases} \tag{26}$$

Note that the Lagrange multiplier $\zeta_h^{j,n+1}$ satisfies $\langle \zeta_h^{j,n+1}, v_h \rangle_{\Gamma_j} = 0, \forall v_h \in S_0^h(\Omega)$.

Next we denote

$$E_h^{j,n+1} = w_h^{j,n+1} - w^{j,n+1}.$$

Then subtracting (26) from (25) and taking $\mu_h = 0$, we have the following error equation:

$$(E_h^{j,n+1}, v_h) + \Delta t a(E_h^{j,n+1}, v_h) - \langle \lambda_h^{j,n+1}, v_h \rangle_{\Gamma_j} = 0, \quad \forall v_h \in S_0^h(\Omega). \tag{27}$$

Lemma 4.2. For the multiplier $\lambda_h^{j,n+1}$ in (25), we have the following result:

$$\|\lambda_h^{j,n+1}\|_{H_h^{-\frac{1}{2}}(\Gamma_j)} \lesssim \|E_h^{j,n+1}\|_{\Omega} + \Delta t \|\nabla E_h^{j,n+1}\|_{\Omega}. \tag{28}$$

Here, $x \lesssim y$ means that $x \leq Cy$ for the constant C that is independent of mesh size and time step size.

Proof. In order to prove this result, we need to define a projection γ^{-1} from $H_h^{\frac{1}{2}}(\Gamma_j)$ to $S_0^h(\Omega)$, similarly to the idea in [19]. First of all, we give two finite element spaces

$$\begin{aligned} S_E^h(\Omega_j) &= \{v \in S^h(\Omega_j) : v|_{\partial\Omega_j \setminus \Gamma_j} = 0\}, \\ S_E^h(\Omega \setminus \Omega_j) &= \{v \in S^h(\Omega \setminus \Omega_j) : v|_{\partial(\Omega \setminus \Omega_j) \setminus \Gamma_j} = 0\}. \end{aligned}$$

Then for any given $g \in H_h^{\frac{1}{2}}(\Gamma_j)$, we define two auxiliary problems

$$a(u_1, v)_{\Omega_j} = 0, \quad u_1|_{\Gamma_j} = g \quad \forall v \in S_0^h(\Omega_j),$$

and

$$a(u_2, v)_{\Omega \setminus \Omega_j} = 0, \quad u_2|_{\Gamma_j} = g \quad \forall v \in S_0^h(\Omega \setminus \Omega_j).$$

Therefore we could define two mapping γ_1^{-1} and γ_2^{-1} from $H_h^{\frac{1}{2}}(\Gamma_j)$ to $S_E^h(\Omega_j)$ and $S_E^h(\Omega \setminus \Omega_j)$, respectively. That is

$$u_1 = \gamma_1^{-1}g, \quad u_2 = \gamma_2^{-1}g.$$

From the regularity results, we have

$$\|\gamma_1^{-1}g\|_{H^1(\Omega_j)} \lesssim \|g\|_{H^{\frac{1}{2}}(\Gamma_j)}, \quad \|\gamma_2^{-1}g\|_{H^1(\Omega \setminus \Omega_j)} \lesssim \|g\|_{H^{\frac{1}{2}}(\Gamma_j)}.$$

Then we can define an operator γ^{-1} as follows: for any given $g \in H_h^{\frac{1}{2}}(\Gamma_j)$,

$$\gamma^{-1}g = \begin{cases} \gamma_1^{-1}g, & \text{in } \Omega_j, \\ \gamma_2^{-1}g, & \text{in } \Omega \setminus \Omega_j. \end{cases}$$

It is easy to obtain the following property of γ^{-1} :

$$\|\gamma^{-1}g\|_{H_0^1(\Omega)} \lesssim \|g\|_{H^{\frac{1}{2}}(\Gamma_j)}, \quad \forall g \in H_h^{\frac{1}{2}}(\Gamma_j). \tag{29}$$

From the definition of $\|\cdot\|_{H_h^{-\frac{1}{2}}(\Gamma_j)}$, (27) and (29), we have

$$\begin{aligned} \|\lambda_h^{j,n+1}\|_{H_h^{-\frac{1}{2}}(\Gamma_j)} &= \sup_{g \in H_h^{\frac{1}{2}}(\Gamma_j)} \frac{\langle \lambda_h^{j,n+1}, g \rangle_{\Gamma_j}}{\|g\|_{H^{\frac{1}{2}}(\Gamma_j)}} \lesssim \sup_{g \in H_h^{\frac{1}{2}}(\Gamma_j)} \frac{\langle \lambda_h^{j,n+1}, \gamma^{-1}g \rangle_{\Gamma_j}}{\|\gamma^{-1}g\|_{H_0^1(\Omega)}} \lesssim \sup_{v_h \in S_0^h(\Omega)} \frac{\langle \lambda_h^{j,n+1}, v_h \rangle_{\Gamma_j}}{\|v_h\|_{H_0^1(\Omega)}} \\ &= \sup_{v_h \in S_0^h(\Omega)} \frac{(E_h^{j,n+1}, v_h) + \Delta t a(E_h^{j,n+1}, v_h)}{\|v_h\|_{H_0^1(\Omega)}} \lesssim \|E_h^{j,n+1}\|_{\Omega} + \Delta t \|\nabla E_h^{j,n+1}\|_{\Omega}. \quad \square \end{aligned}$$

Lemma 4.3. Assume $w^{j,n+1}$, $j = 1, \dots, M$, $n = 0, \dots, N - 1$, is the solution of (16), then we have

$$\|E_h^{j,n+1}\|_{\Omega}^2 + \Delta t \|\nabla E_h^{j,n+1}\|_{\Omega}^2 \lesssim \|w^{j,n+1}\|_{\Omega}^2 + \Delta t \|\nabla w^{j,n+1}\|_{\Omega}^2. \tag{30}$$

Proof. From the definition of $E_h^{j,n+1}$ and $w^{j,n+1}$, we have

$$E_h^{j,n+1}|_{\Omega_j} = w^{j,n+1} - w_h^{j,n+1} \quad \text{and} \quad E_h^{j,n+1}|_{\Omega \setminus \Omega_j} = w^{j,n+1}.$$

Then considering the local error equation (27) leads to

$$\begin{cases} (E_h^{j,n+1}, v_h) + \Delta t a(E_h^{j,n+1}, v_h) = 0, & \forall v_h \in S_0^h(\Omega_j), \\ E_h^{j,n+1}|_{\partial\Omega_j} = w^{j,n+1}. \end{cases} \tag{31}$$

Thus we derive

$$\|E_h^{j,n+1}\|_{\Omega_j}^2 + \Delta t \|\nabla E_h^{j,n+1}\|_{\Omega_j}^2 \leq \Delta t \|w^{j,n+1}\|_{H^{\frac{1}{2}}(\partial\Omega_j)}^2.$$

Since $w^{j,n+1} \in S_0^h(\Omega)$, we have

$$\|E_h^{j,n+1}\|_{\Omega_j}^2 + \Delta t \|\nabla E_h^{j,n+1}\|_{\Omega_j}^2 \lesssim \Delta t \|w^{j,n+1}\|_{H^{\frac{1}{2}}(\partial\Omega_j)}^2 = \Delta t \|w^{j,n+1}\|_{H^{\frac{1}{2}}(\partial(\Omega \setminus \Omega_j))}^2 \lesssim \Delta t \|\nabla w^{j,n+1}\|_{\Omega \setminus \Omega_j}^2.$$

Hence

$$\begin{aligned} \|E_h^{j,n+1}\|_{\Omega}^2 + \Delta t \|\nabla E_h^{j,n+1}\|_{\Omega}^2 &= \|E_h^{j,n+1}\|_{\Omega_j}^2 + \Delta t \|\nabla E_h^{j,n+1}\|_{\Omega_j}^2 + \|w^{j,n+1}\|_{\Omega \setminus \Omega_j}^2 + \Delta t \|\nabla w^{j,n+1}\|_{\Omega \setminus \Omega_j}^2 \\ &\lesssim \Delta t \|\nabla w^{j,n+1}\|_{\Omega \setminus \Omega_j}^2 + \|w^{j,n+1}\|_{\Omega \setminus \Omega_j}^2 + \Delta t \|\nabla w^{j,n+1}\|_{\Omega \setminus \Omega_j}^2 \\ &\lesssim \|w^{j,n+1}\|_{\Omega \setminus \Omega_j}^2 + \Delta t \|\nabla w^{j,n+1}\|_{\Omega \setminus \Omega_j}^2 \\ &\lesssim \|w^{j,n+1}\|_{\Omega}^2 + \Delta t \|\nabla w^{j,n+1}\|_{\Omega}^2. \end{aligned}$$

Thus we complete the proof. \square

Lemma 4.4. If $w^{j,n+1}$, $j = 1, \dots, M$, $n = 1, \dots, N - 1$ is the solution of (16), we have

$$\|w^{j,n+1}\|_{\Omega}^2 + \Delta t \|\nabla w^{j,n+1}\|_{\Omega}^2 \lesssim \Delta t^4 \|S_{1,h}^{n+1}\|_{D_j}^2 + \Delta t^3 \int_{t^{n-1}}^{t^{n+1}} \|u_n\|_{D_j}^2 dt. \tag{32}$$

Proof. Considering (16) and (12), we can obtain

$$\begin{aligned} \left(\frac{w^{j,n+1}}{\Delta t}, v_h\right) + a(w^{j,n+1}, v_h) &= -\left(\frac{u^{n+1} - u^n}{\Delta t}, \phi_j v_h\right) - a(u^{n+1}, \phi_j v_h) + a\left(\frac{u^{n+1} - u^n}{2}, \phi_j v_h\right) + \left(\frac{f^{n+1} + f^n}{2}, \phi_j v_h\right) \\ &= -(f^{n+1}, \phi_j v_h) + a\left(\frac{u^{n+1} - u^n}{2}, \phi_j v_h\right) + \left(\frac{f^{n+1} + f^n}{2}, \phi_j v_h\right) \\ &= a\left(\frac{u^{n+1} - u^n}{2}, \phi_j v_h\right) - \left(\frac{f^{n+1} - f^n}{2}, \phi_j v_h\right) \\ &= -\frac{1}{2}\left(\frac{u^{n+1} - u^n}{\Delta t} - \frac{u^n - u^{n-1}}{\Delta t}, \phi_j v_h\right) \\ &= \frac{1}{2}\Delta t(S_{1,h}^{n+1}, \phi_j v_h) - \frac{1}{2}\left(\frac{u^{n+1} - u^n}{\Delta t} - \frac{u^n - u^{n-1}}{\Delta t}, \phi_j v_h\right). \end{aligned}$$

Taking $v_h = \Delta t w^{j,n+1}$ in the above equation, we get

$$\|w^{j,n+1}\|_{\Omega}^2 + \Delta t \|\nabla w^{j,n+1}\|_{\Omega}^2 = \Delta t^2(S_{1,h}^{n+1}, \phi_j w^{j,n+1}) - \Delta t\left(\frac{u^{n+1} - u^n}{\Delta t} - \frac{u^n - u^{n-1}}{\Delta t}, \phi_j w^{j,n+1}\right).$$

Then using the Hölder and Young’s inequalities, we have

$$\Delta t^2(S_{1,h}^{n+1}, \phi_j w^{j,n+1}) \leq \Delta t^2 \|S_{1,h}^{n+1}\|_{D_j} \|w^{j,n+1}\|_{D_j} \leq \frac{1}{4} \|w^{j,n+1}\|_{D_j}^2 + \Delta t^4 \|S_{1,h}^{n+1}\|_{D_j}^2,$$

and

$$\begin{aligned} \Delta t\left(\frac{u^{n+1} - u^n}{\Delta t} - \frac{u^n - u^{n-1}}{\Delta t}, \phi_j w^{j,n+1}\right) &\leq \Delta t \left\| \frac{u^{n+1} - u^n}{\Delta t} - \frac{u^n - u^{n-1}}{\Delta t} \right\|_{D_j} \|w^{j,n+1}\|_{D_j} \\ &\leq \frac{1}{4} \|w^{j,n+1}\|_{D_j}^2 + \Delta t^2 \left\| \frac{u^{n+1} - u^n}{\Delta t} - \frac{u^n - u^{n-1}}{\Delta t} \right\|_{D_j}^2. \end{aligned}$$

In addition, considering the Taylor series with the integral remainder, we can obtain

$$\begin{aligned} u^{n+1} &= u^n + \Delta t u_t^n + \int_{t^n}^{t^{n+1}} (t^{n+1} - t) u_{tt} dt, \\ u^{n-1} &= u^n - \Delta t u_t^n + \int_{t^n}^{t^{n-1}} (t^{n-1} - t) u_{tt} dt. \end{aligned}$$

So we have

$$u^{n+1} - 2u^n + u^{n-1} = \int_{t^n}^{t^{n+1}} (t^{n+1} - t) u_{tt} dt + \int_{t^{n-1}}^{t^n} (t - t^{n-1}) u_{tt} dt.$$

Using the Minkowski and Hölder inequalities yields

$$\begin{aligned} \|u^{n+1} - 2u^n + u^{n-1}\|_{D_j}^2 &\leq \left(\left\| \int_{t^n}^{t^{n+1}} (t^{n+1} - t) u_{tt} dt \right\|_{D_j} + \left\| \int_{t^{n-1}}^{t^n} (t - t^{n-1}) u_{tt} dt \right\|_{D_j} \right)^2 \\ &\leq 2 \left\| \int_{t^n}^{t^{n+1}} (t^{n+1} - t) u_{tt} dt \right\|_{D_j}^2 + 2 \left\| \int_{t^{n-1}}^{t^n} (t - t^{n-1}) u_{tt} dt \right\|_{D_j}^2 \\ &\leq 2 \int_{t^n}^{t^{n+1}} (t^{n+1} - t)^2 dt \int_{t^n}^{t^{n+1}} \|u_{tt}\|_{D_j}^2 dt + 2 \int_{t^{n-1}}^{t^n} (t - t^{n-1})^2 dt \int_{t^{n-1}}^{t^n} \|u_{tt}\|_{D_j}^2 dt \\ &\leq C \Delta t^3 \int_{t^{n-1}}^{t^{n+1}} \|u_{tt}\|_{D_j}^2 dt. \end{aligned}$$

Hence,

$$\|w^{j,n+1}\|_{\Omega}^2 + \Delta t \|\nabla w^{j,n+1}\|_{\Omega}^2 \leq C \Delta t^4 \|S_{1,h}^{n+1}\|_{D_j}^2 + C \Delta t^3 \int_{t^{n-1}}^{t^{n+1}} \|u_{tt}\|_{D_j}^2 dt.$$

Thus, we complete this proof. \square

Theorem 4.1. Assume that $u_{2,h}^m$, $m = 1, \dots, N$, is obtained by Algorithm 3.1. Under the assumptions (21) and (23), we have

$$\|u_{2,h}^m\|_{\Omega}^2 + \Delta t \sum_{n=0}^{m-1} \|\nabla u_{2,h}^{n+1}\|_{\Omega}^2 \lesssim 1 + \Delta t \sum_{n=0}^m \|f^n\|_{\Omega}^2. \tag{33}$$

Proof. Since $\sum_{j=1}^M \phi_j = 1$ and $w_h^{n+1} = \sum_{j=1}^M w_h^{j,n+1}$, taking $\mu_h = 0$ in (25) and summing it from $j = 1$ to M lead to $\forall v_h \in S_0^h(\Omega)$,

$$\left(\frac{w_h^{n+1}}{\Delta t}, v_h\right) + a(w_h^{n+1}, v_h) = \frac{1}{\Delta t} \sum_{j=1}^M \int_{\Gamma_j} \lambda_h^{j,n+1} v_h ds - \left(\frac{u_{1,h}^{n+1} - u_{1,h}^n}{\Delta t}, v_h\right) - a(u_{1,h}^{n+1}, v_h) + a\left(\frac{u_{1,h}^{n+1} - u_{1,h}^n}{2}, v_h\right) + \left(\frac{f^{n+1} + f^n}{2}, v_h\right).$$

Since $u_F^{n+1} = w_h^{n+1} + u_{1,h}^{n+1} \in S_0^h(\Omega)$, we obtain

$$\left(\frac{u_F^{n+1} - u_{1,h}^n}{\Delta t}, v_h\right) + a(u_F^{n+1}, v_h) = \frac{1}{\Delta t} \sum_{j=1}^M \int_{\Gamma_j} \lambda_h^{j,n+1} v_h ds + a\left(\frac{u_{1,h}^{n+1} - u_{1,h}^n}{2}, v_h\right) + \left(\frac{f^{n+1} + f^n}{2}, v_h\right). \tag{34}$$

Notice that the final approximate solution $u_{2,h}^{n+1} = u_G^{n+1} + u_F^{n+1} - u_{1,h}^{n+1} \in S_0^h(\Omega)$. Considering (18), (34) and (12), we obtain

$$\left(\frac{u_{2,h}^{n+1} - u_{2,h}^n}{\Delta t}, v_h\right) + a(u_{2,h}^{n+1}, v_h) = \frac{1}{\Delta t} \sum_{j=1}^M \int_{\Gamma_j} \lambda_h^{j,n+1} v_h ds + a\left(\frac{u_{1,h}^{n+1} - u_{1,h}^n}{2}, v_h\right) + \left(\frac{f^{n+1} + f^n}{2}, v_h\right). \tag{35}$$

Taking $v_h = 2\Delta t u_{2,h}^{n+1} \in S_0^h(\Omega)$ and using the equality

$$2(x - y, x) = |x|^2 - |y|^2 + |x - y|^2, \quad \forall x, y \in \mathbb{R}^d, \tag{36}$$

we can get

$$\|u_{2,h}^{n+1}\|_{\Omega}^2 - \|u_{2,h}^n\|_{\Omega}^2 + \|u_{2,h}^{n+1} - u_{2,h}^n\|_{\Omega}^2 + 2\Delta t \|\nabla u_{2,h}^{n+1}\|_{\Omega}^2 = 2 \sum_{j=1}^M \int_{\Gamma_j} \lambda_h^{j,n+1} u_{2,h}^{n+1} ds + \Delta t a(u_{1,h}^{n+1} - u_{1,h}^n, u_{2,h}^{n+1}) + \Delta t (f^{n+1} + f^n, u_{2,h}^{n+1}). \tag{37}$$

For the first term on the right hand side, using the Hölder, Cauchy-Schwarz and Young’s inequalities yield

$$\begin{aligned} 2 \sum_{j=1}^M \int_{\Gamma_j} \lambda_h^{j,n+1} u_{2,h}^{n+1} ds &\leq \sum_{j=1}^M \|\lambda_h^{j,n+1}\|_{H^{-\frac{1}{2}}(\Gamma_j)} \|u_{2,h}^{n+1}\|_{H^{\frac{1}{2}}(\Gamma_j)} \leq \sum_{j=1}^M \|\lambda_h^{j,n+1}\|_{H^{-\frac{1}{2}}(\Gamma_j)} \|u_{2,h}^{n+1}\|_{H^1(\Omega_j)} \\ &\leq \left(\sum_{j=1}^M \|\lambda_h^{j,n+1}\|_{H^{-\frac{1}{2}}(\Gamma_j)}^2\right)^{\frac{1}{2}} \left(\sum_{j=1}^M \|u_{2,h}^{n+1}\|_{H^1(\Omega_j)}^2\right)^{\frac{1}{2}} \\ &\leq \kappa^{\frac{1}{2}} \left(\sum_{j=1}^M \|\lambda_h^{j,n+1}\|_{H^{-\frac{1}{2}}(\Gamma_j)}^2\right)^{\frac{1}{2}} \|u_{2,h}^{n+1}\|_{H^1(\Omega)} \\ &\leq \varepsilon \Delta t \|\nabla u_{2,h}^{n+1}\|_{\Omega}^2 + \frac{C\kappa}{\varepsilon \Delta t} \sum_{j=1}^M \|\lambda_h^{j,n+1}\|_{H^{-\frac{1}{2}}(\Gamma_j)}^2. \end{aligned}$$

Here a positive integer κ independent of M and $x \in \Omega$, is the maximum number of sub-domain Ω_j which includes the point x . For the remain terms on the right hand sides of (37), using the Hölder and Young’s inequalities lead to

$$\begin{aligned} \Delta t a(u_{1,h}^{n+1} - u_{1,h}^n, u_{2,h}^{n+1}) &\leq \Delta t (\|\nabla u_{1,h}^{n+1}\|_{\Omega} + \|\nabla u_{1,h}^n\|_{\Omega}) \|\nabla u_{2,h}^{n+1}\|_{\Omega} \\ &\leq 2\varepsilon \Delta t \|\nabla u_{2,h}^{n+1}\|_{\Omega}^2 + \frac{1}{4\varepsilon} \Delta t (\|\nabla u_{1,h}^{n+1}\|_{\Omega}^2 + \|\nabla u_{1,h}^n\|_{\Omega}^2), \end{aligned}$$

and using the Poincaré inequality gets

$$\begin{aligned} \Delta t (f^{n+1} + f^n, u_{2,h}^{n+1}) &\leq \Delta t (\|f^{n+1}\|_{\Omega} + \|f^n\|_{\Omega}) \|u_{2,h}^{n+1}\|_{\Omega} \leq C_p \Delta t (\|f^{n+1}\|_{\Omega} + \|f^n\|_{\Omega}) \|\nabla u_{2,h}^{n+1}\|_{\Omega} \\ &\leq 2\varepsilon \Delta t \|\nabla u_{2,h}^{n+1}\|_{\Omega}^2 + \frac{C_p^2}{4\varepsilon} \Delta t (\|f^{n+1}\|_{\Omega}^2 + \|f^n\|_{\Omega}^2). \end{aligned}$$

Combining the above estimations with (37) and setting $\varepsilon = 1/5$, we obtain

$$\|u_{2,h}^{n+1}\|_{\Omega}^2 - \|u_{2,h}^n\|_{\Omega}^2 + \Delta t \|\nabla u_{2,h}^{n+1}\|_{\Omega}^2 \leq \frac{5C\kappa}{\Delta t} \sum_{j=1}^M \|\lambda_h^{j,n+1}\|_{H^{-\frac{1}{2}}(\Gamma_j)}^2 + \frac{5}{4} \Delta t \|\nabla u_{1,h}^{n+1}\|_{\Omega}^2 + \frac{5}{4} \Delta t \|\nabla u_{1,h}^n\|_{\Omega}^2 + \frac{5}{4} C_p^2 \Delta t \|f^{n+1}\|_{\Omega}^2 + \frac{5}{4} C_p^2 \Delta t \|f^n\|_{\Omega}^2.$$

Considering $u_{2,h}^0 = 0$ and summing the above equation from $n = 0$ to $n = m - 1$, we get

$$\|u_{2,h}^m\|_{\Omega}^2 + \Delta t \sum_{n=0}^{m-1} \|\nabla u_{2,h}^{n+1}\|_{\Omega}^2 \leq \frac{5C\kappa}{\Delta t} \sum_{n=0}^{m-1} \sum_{j=1}^M \|\lambda_h^{j,n+1}\|_{H^{-\frac{1}{2}}(\Gamma_j)}^2 + \frac{5}{2} \Delta t \sum_{n=0}^m \|\nabla u_{1,h}^n\|_{\Omega}^2 + \frac{5}{2} C_p^2 \Delta t \sum_{n=0}^m \|f^n\|_{\Omega}^2.$$

Then using (21), (24), (28), (30), (32) and the Young’s inequality, we have

$$\begin{aligned}
 \frac{\kappa}{\Delta t} \sum_{n=0}^{m-1} \sum_{j=1}^M \|\lambda_h^{j,n+1}\|_{H_h^{-\frac{1}{2}}(\Gamma_j)}^2 &\lesssim \frac{\kappa}{\Delta t} \sum_{n=0}^{m-1} \sum_{j=1}^M \left(\Delta t^4 \|S_{1,h}^{n+1}\|_{D_j}^2 + \Delta t^3 \int_{t^{n-1}}^{t^{n+1}} \|u_{tt}\|_{D_j}^2 dt \right) \\
 &\lesssim \frac{\kappa}{\Delta t} \sum_{n=0}^{m-1} \left(\Delta t^4 \|S_{1,h}^{n+1}\|_{\Omega}^2 + \Delta t^3 \int_{t^{n-1}}^{t^{n+1}} \|u_{tt}\|_{\Omega}^2 dt \right) \\
 &\lesssim \kappa \sum_{n=0}^{m-1} \Delta t^3 \|S_{1,h}^{n+1}\|_{\Omega}^2 + \kappa \Delta t^2 \sum_{n=0}^{m-1} \int_{t^{n-1}}^{t^{n+1}} \|u_{tt}\|_{\Omega}^2 dt \\
 &\lesssim \Delta t^2 (\Delta t^2 + h^{2r}) + \Delta t^2 \|u_{tt}\|_{L^2(0,T;L^2(\Omega))}^2 \\
 &\lesssim \Delta t^2 + h^{2r+2} \lesssim 1.
 \end{aligned} \tag{38}$$

From the stability result (20), we can obtain the final result (33). \square

5. The error analysis

We decompose the error between the true solution u^{n+1} and the numerical solution $u_{2,h}^{n+1}$ of Algorithm 3.1 into the numerical error and the approximate error as follows:

$$u_{2,h}^{n+1} - u^{n+1} = (u_{2,h}^{n+1} - P_h u^{n+1}) - (u^{n+1} - P_h u^{n+1}) := e_{2,h}^{n+1} - \xi_h^{n+1}.$$

According to these symbols, in the following proof process, an error equation is first constructed. Then the final convergence result is obtained by appropriate estimations.

Theorem 5.1. Assume that $u_{2,h}^m$, $m = 1, \dots, N$, is obtained by Algorithm 3.1. Under the assumptions (21), (23) and $\Delta t \leq h^{r+1}$, we have the following result

$$\|u_{2,h}^m - u^m\|_{\Omega}^2 \leq C(\Delta t^4 + h^{2r+2}). \tag{39}$$

Proof. If we take the average of (2) at time $t = t^n$ and $t = t^{n+1}$, $n = 0, \dots, N - 1$, we obtain

$$\left(\frac{u_t^{n+1} + u_t^n}{2}, v \right) + a\left(\frac{u^{n+1} + u^n}{2}, v \right) = \left(\frac{f^{n+1} + f^n}{2}, v \right), \quad \forall v \in H_0^1(\Omega).$$

It is easy to obtain

$$\left(\frac{u^{n+1} - u^n}{\Delta t}, v \right) + a(u^{n+1}, v) = \left(\frac{u^{n+1} - u^n}{\Delta t} - \frac{u_t^{n+1} + u_t^n}{2}, v \right) + a\left(\frac{u^{n+1} - u^n}{2}, v \right) + \left(\frac{f^{n+1} + f^n}{2}, v \right). \tag{40}$$

Then taking $v = v_h$ in (40) and subtracting it from (35), we have

$$\left(\frac{e_{2,h}^{n+1} - e_{2,h}^n}{\Delta t}, v_h \right) + a(e_{2,h}^{n+1}, v_h) = \left(\frac{\xi_h^{n+1} - \xi_h^n}{\Delta t}, v_h \right) + a(\xi_h^{n+1}, v_h) + \frac{1}{\Delta t} \sum_{j=1}^M \int_{\Gamma_j} \lambda_h^{j,n+1} v_h ds + \left(\frac{u_t^{n+1} - u_t^n}{\Delta t} - \frac{u^{n+1} + u^n}{2}, v_h \right) + a\left(\frac{e_{1,h}^{n+1} - e_{1,h}^n}{2}, v_h \right). \tag{41}$$

Considering the definition of P_h (3) leads to

$$a(\xi_h^{n+1}, v_h) = 0.$$

Taking $v_h = 2\Delta t e_{2,h}^{n+1} \in S_0^h(\Omega)$ in (41) and using (36), we obtain

$$\begin{aligned}
 &\|e_{2,h}^{n+1}\|_{\Omega}^2 - \|e_{2,h}^n\|_{\Omega}^2 + \|e_{2,h}^{n+1} - e_{2,h}^n\|_{\Omega}^2 + 2\Delta t \|\nabla e_{2,h}^{n+1}\|_{\Omega}^2 \\
 &= 2\Delta t \left(\frac{\xi_h^{n+1} - \xi_h^n}{\Delta t}, e_{2,h}^{n+1} \right) + 2 \sum_{j=1}^M \int_{\Gamma_j} \lambda_h^{j,n+1} e_{2,h}^{n+1} ds + 2\Delta t \left(\frac{u_t^{n+1} - u_t^n}{\Delta t} - \frac{u^{n+1} + u^n}{2}, e_{2,h}^{n+1} \right) + \Delta t^2 a(d_t e_{1,h}^{n+1}, e_{2,h}^{n+1}).
 \end{aligned} \tag{42}$$

Using the Hölder, Poincaré (5) and Young’s (6) inequalities, we have

$$\begin{aligned}
 2\Delta t \left(\frac{\xi_h^{n+1} - \xi_h^n}{\Delta t}, e_{2,h}^{n+1} \right) &\leq 2C_p \Delta t \left\| \frac{\xi_h^{n+1} - \xi_h^n}{\Delta t} \right\|_{\Omega} \|\nabla e_{2,h}^{n+1}\|_{\Omega} \\
 &\leq \varepsilon \Delta t \|\nabla e_{2,h}^{n+1}\|_{\Omega}^2 + \frac{C_p^2}{\varepsilon} \Delta t \left\| \frac{\xi_h^{n+1} - \xi_h^n}{\Delta t} \right\|_{\Omega}^2.
 \end{aligned}$$

For the second term on the right hand side of (41), by using the Hölder, Cauchy-Schwarz and Young’s inequalities, we have

$$\begin{aligned}
 2 \sum_{j=1}^M \int_{\Gamma_j} \lambda_h^{j,n+1} e_{2,h}^{n+1} ds &\lesssim \sum_{j=1}^M \|\lambda_h^{j,n+1}\|_{H^{-\frac{1}{2}}(\Gamma_j)} \|e_{2,h}^{n+1}\|_{H^{\frac{1}{2}}(\Gamma_j)} \leq \sum_{j=1}^M \|\lambda_h^{j,n+1}\|_{H^{-\frac{1}{2}}(\Gamma_j)} \|e_{2,h}^{n+1}\|_{H^1(\Omega_j)} \\
 &\lesssim \left(\sum_{j=1}^M \|\lambda_h^{j,n+1}\|_{H^{-\frac{1}{2}}(\Gamma_j)}^2 \right)^{\frac{1}{2}} \left(\sum_{j=1}^M \|e_{2,h}^{n+1}\|_{H^1(\Omega_j)}^2 \right)^{\frac{1}{2}} \\
 &\lesssim \kappa^{\frac{1}{2}} \left(\sum_{j=1}^M \|\lambda_h^{j,n+1}\|_{H^{-\frac{1}{2}}(\Gamma_j)}^2 \right)^{\frac{1}{2}} \|e_{2,h}^{n+1}\|_{H^1(\Omega)} \\
 &\leq \varepsilon \Delta t \|\nabla e_{2,h}^{n+1}\|_{\Omega}^2 + \frac{C\kappa}{\varepsilon \Delta t} \sum_{j=1}^M \|\lambda_h^{j,n+1}\|_{H^{-\frac{1}{2}}(\Gamma_j)}^2.
 \end{aligned}$$

Here a positive integer κ independent of M and $x \in \Omega$, is the maximum number of sub-domain Ω_j which includes the point x . Then using Poincaré, Hölder and Young’s inequalities, we have

$$\begin{aligned}
 2\Delta t \left(\frac{u_t^{n+1} + u_t^n}{2} - \frac{u^{n+1} - u^n}{\Delta t}, e_{2,h}^{n+1} \right) &\leq 2C_p \Delta t \left\| \frac{u_t^{n+1} + u_t^n}{2} - \frac{u^{n+1} - u^n}{\Delta t} \right\|_{\Omega} \|\nabla e_{2,h}^{n+1}\|_{\Omega} \\
 &\leq \varepsilon \Delta t \|\nabla e_{2,h}^{n+1}\|_{\Omega}^2 + \frac{C_p^2}{\varepsilon} \Delta t \left\| \frac{u_t^{n+1} + u_t^n}{2} - \frac{u^{n+1} - u^n}{\Delta t} \right\|_{\Omega}^2,
 \end{aligned}$$

and

$$\begin{aligned}
 \Delta t^2 a(d_t e_{1,h}^{n+1}, e_{2,h}^{n+1}) &\leq \Delta t^2 \|\nabla d_t e_{1,h}^{n+1}\|_{\Omega} \|\nabla e_{2,h}^{n+1}\|_{\Omega} \\
 &\leq \varepsilon \Delta t \|\nabla e_{2,h}^{n+1}\|_{\Omega}^2 + \frac{1}{4\varepsilon} \Delta t^3 \|\nabla d_t e_{1,h}^{n+1}\|_{\Omega}^2.
 \end{aligned}$$

Combining the above estimates with (42) and setting $\varepsilon = 1/4$, we derive

$$\begin{aligned}
 &\|e_{2,h}^{n+1}\|_{\Omega}^2 - \|e_{2,h}^n\|_{\Omega}^2 + \|e_{2,h}^{n+1} - e_{2,h}^n\|_{\Omega}^2 + \Delta t \|\nabla e_{2,h}^{n+1}\|_{\Omega}^2 \\
 &\leq 4C_p^2 \Delta t \left\| \frac{\xi_h^{n+1} - \xi_h^n}{\Delta t} \right\|_{\Omega}^2 + \frac{C\kappa}{\Delta t} \sum_{j=1}^M \|\lambda_h^{j,n+1}\|_{H^{-\frac{1}{2}}(\Gamma_j)}^2 + 4C_p^2 \Delta t \left\| \frac{u_t^{n+1} + u_t^n}{2} - \frac{u^{n+1} - u^n}{\Delta t} \right\|_{\Omega}^2 + \Delta t^3 \|\nabla d_t e_{1,h}^{n+1}\|_{\Omega}^2.
 \end{aligned}$$

From the Hölder’s inequality, we obtain

$$\left\| \frac{\xi_h^{n+1} - \xi_h^n}{\Delta t} \right\|_{\Omega}^2 = \left\| \frac{1}{\Delta t} \int_{t^n}^{t^{n+1}} 1 \cdot (\xi_h)_t dt \right\|_{\Omega}^2 \leq \frac{C}{\Delta t} \int_{t^n}^{t^{n+1}} \|(\xi_h)_t\|_{\Omega}^2 dt,$$

and

$$\begin{aligned}
 \left\| \frac{u_t^{n+1} + u_t^n}{2} - \frac{u^{n+1} - u^n}{\Delta t} \right\|_{\Omega}^2 &= \left\| \frac{1}{\Delta t} \int_{t^n}^{t^{n+1}} u_t dt - \frac{u_t^{n+1} + u_t^n}{2} \right\|_{\Omega}^2 \\
 &\leq \left\| \frac{1}{2\Delta t} \int_{t^n}^{t^{n+1}} (t - t^n)(t - t^{n+1}) u_{ttt} dt \right\|_{\Omega}^2 \\
 &\leq \frac{C}{\Delta t^2} \int_{t^n}^{t^{n+1}} (t - t^n)^2 (t - t^{n+1})^2 dt \int_{t^n}^{t^{n+1}} \|u_{ttt}\|_{\Omega}^2 dt \\
 &\leq C \Delta t^3 \int_{t^n}^{t^{n+1}} \|u_{ttt}\|_{\Omega}^2 dt.
 \end{aligned}$$

So that

$$\begin{aligned}
 &\|e_{2,h}^{n+1}\|_{\Omega}^2 - \|e_{2,h}^n\|_{\Omega}^2 + \|e_{2,h}^{n+1} - e_{2,h}^n\|_{\Omega}^2 + \Delta t \|\nabla e_{2,h}^{n+1}\|_{\Omega}^2 \\
 &\leq C \int_{t^n}^{t^{n+1}} \|(\xi_h)_t\|_{\Omega}^2 dt + \frac{C\kappa}{\Delta t} \sum_{j=1}^M \|\lambda_h^{j,n+1}\|_{H^{-\frac{1}{2}}(\Gamma_j)}^2 + C \Delta t^4 \int_{t^n}^{t^{n+1}} \|u_{ttt}\|_{\Omega}^2 dt + \Delta t^3 \|\nabla d_t e_{1,h}^{n+1}\|_{\Omega}^2.
 \end{aligned}$$

Note that $e_{2,h}^0 = 0$, then summing the above equation from $n = 0$ to $n = m - 1$ and considering (4) and (21) yield

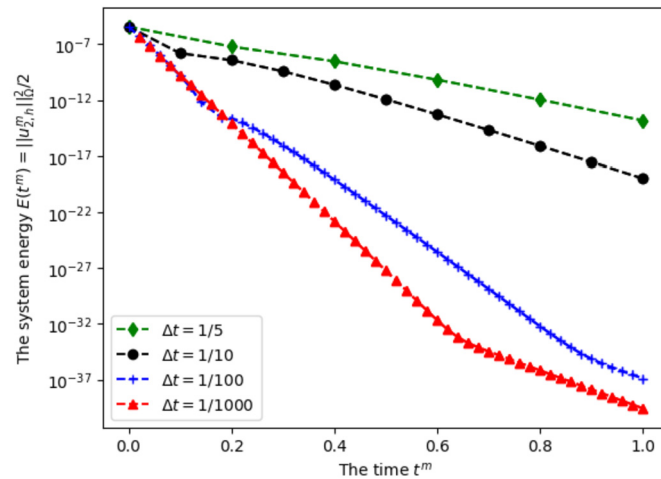


Fig. 1. The system energy changes of Algorithm 3.1 with different time steps Δt and fixed mesh size $h = 1/32$.

$$\begin{aligned}
 & \|e_{2,h}^m\|_{\Omega}^2 + \|e_{2,h}^{n+1} - e_{2,h}^n\|_{\Omega}^2 + \Delta t \sum_{n=0}^m \|\nabla e_{2,h}^{n+1}\|_{\Omega}^2 \\
 & \leq C \sum_{n=0}^m \int_{t^n}^{t^{n+1}} \|(\xi_h)_t\|_{\Omega}^2 dt + \frac{CK}{\Delta t} \sum_{n=0}^m \sum_{j=1}^M \|\lambda_h^{j,n+1}\|_{H_h^{-\frac{1}{2}}(\Gamma_j)}^2 + C\Delta t^4 \sum_{n=0}^m \int_{t^n}^{t^{n+1}} \|u_{ttt}\|_{\Omega}^2 dt + \Delta t^3 \sum_{n=0}^m \|\nabla d_t e_{1,h}^{n+1}\|_{\Omega}^2 \\
 & \leq C \int_0^T \|(\xi_h)_t\|_{\Omega}^2 dt + \frac{CK}{\Delta t} \sum_{n=0}^m \sum_{j=1}^M \|\lambda_h^{j,n+1}\|_{H_h^{-\frac{1}{2}}(\Gamma_j)}^2 + C\Delta t^4 \int_0^T \|u_{ttt}\|_{\Omega}^2 dt + \Delta t^3 \sum_{n=0}^m \|\nabla d_t e_{1,h}^{n+1}\|_{\Omega}^2 \\
 & \leq Ch^{2r+2} \|u_t\|_{L^2(0,T;H^{r+1}(\Omega))}^2 + \frac{CK}{\Delta t} \sum_{n=0}^m \sum_{j=1}^M \|\lambda_h^{j,n+1}\|_{H_h^{-\frac{1}{2}}(\Gamma_j)}^2 + C\Delta t^4 \|u_{ttt}\|_{L^2(0,T;L^2(\Omega))}^2 + \Delta t^3 \sum_{n=0}^m \|\nabla d_t e_{1,h}^{n+1}\|_{\Omega}^2.
 \end{aligned}$$

From (38) and the assumption $\Delta t \leq h^{r+1}$, we have

$$\frac{K}{\Delta t} \sum_{n=0}^{m-1} \sum_{j=1}^M \|\lambda_h^{j,n+1}\|_{H_h^{-\frac{1}{2}}(\Gamma_j)}^2 \leq C(\Delta t^2 + h^{2r+2}) \leq Ch^{2r+2}.$$

From (22), we have

$$\Delta t^3 \sum_{n=0}^m \|\nabla d_t e_{1,h}^{n+1}\|_{\Omega}^2 \leq C\Delta t^2(\Delta t^2 + h^{2r}) \leq C(\Delta t^4 + h^{2r+2}).$$

Considering (4) and using the triangle inequality, we obtain the final result. \square

6. Numerical experiments

In this section, we present some 2D numerical experiments to confirm the effectiveness of our local and parallel space-time scheme. All codes are implemented by using the software package FreeFem++ [35]. Experiment 1 and Experiment 2 respectively verify the stability and convergence of Algorithm 3.1. For other experiments, we further verify the effectiveness of our space-time parallel algorithm.

6.1. Experiment 1: the stability

Let the computational domain be the unit square $\Omega = (0, 1) \times (0, 1)$ with the uniform triangulation $T^h(\Omega) = \{\tau_{\Omega}^h\}$. For the finite element spaces, we choose the piecewise linear finite element spaces as follows:

$$S^h(\Omega) = \{v \in C^0(\Omega) : v|_{\tau_{\Omega}^h} \in P_{\tau_{\Omega}^h}^1, \forall \tau_{\Omega}^h \in T^h(\Omega)\}.$$

In this experiment, we assume the density of heat source $f = 0$ and the initial value of temperature

$$u(0) = (x^4 - 2x^3 + x^2)(2y^3 - 3y^2 + y).$$

To verify the stability of Algorithm 3.1, we define the system energy $E(t^m) = \frac{1}{2} \|u_{2,h}^m\|_{\Omega}^2$. However, for a system with no energy exchange and no external force, the system energy would decay with time. So we test the stability of Algorithm 3.1 by calculating the system energy and observing whether the energy decays with $f = 0$. Let us choose different time steps $\Delta t = 1/5, 1/10, 1/100, 1/1000$ and the fixed mesh size $h = 1/32$. What's more, we choose another grid triangulation $T^H(\Omega)$ with $H = 1/8$ to obtain the partition of unity on Ω and the local computational domain Ω_j . Then we calculate the system energy $E(t^m)$ at time $t^m \in [0, 1]$. We show the variable trend of system energy in Fig. 1, which illustrates the stability of Algorithm 3.1.

Table 1

The convergence orders with respect to the time step Δt at time $t^m = 1$, with the fixed mesh size $h = 1/16$.

Δt	$\ u_{2,h}^{m,\Delta t} - u_{2,h}^{m,\frac{\Delta t}{2}}\ _{\Omega}$	$\rho_{u_{2,h}^{m,\Delta t},0}$	Order
1/5	9.981e-5	4.179	2.063
1/10	2.115e-5	4.636	2.213
1/20	4.562e-6		

Table 2

The convergence orders with respect to the mesh size h at time $t_m = 1$, with the fixed time step length $\Delta t = 1/10$.

h	$\ u_{2,h}^{m,h} - u_{2,h}^{m,\frac{h}{2}}\ _{\Omega}$	$\rho_{u_{2,h}^{m,h},0}$	Order
1/8	1.194e-5	6.742	2.753
1/16	1.771e-6	10.12	3.339
1/32	1.750e-7		

6.2. Experiment 2: the order of convergence

To examine the orders of convergence with respect to the time step Δt or the mesh size h , we give the following measure of the convergence. If we assume that

$$u_h^{\Delta t}(x, t_m) \approx u(x, t_m) + C_1(x, t_m)\Delta t^{\gamma} + C_2(x, t_m)h^{\mu},$$

where γ and μ are positive constants. Then the measures testing the convergence order of the time step Δt and the mesh size h are defined as follows:

$$\begin{aligned} \rho_{u,\Delta t,0} &= \frac{\|u_h^{\Delta t}(x, t_m) - u_h^{\frac{\Delta t}{2}}(x, t_m)\|_0}{\|u_h^{\frac{\Delta t}{2}}(x, t_m) - u_h^{\frac{\Delta t}{4}}(x, t_m)\|_0} \approx \frac{4^{\gamma} - 2^{\gamma}}{2^{\gamma} - 1}, \\ \rho_{u,h,0} &= \frac{\|u_h^{\Delta t}(x, t_m) - u_h^{\frac{\Delta t}{2}}(x, t_m)\|_0}{\|u_h^{\Delta t}(x, t_m) - u_h^{\frac{\Delta t}{4}}(x, t_m)\|_0} \approx \frac{4^{\mu} - 2^{\mu}}{2^{\mu} - 1}. \end{aligned} \tag{43}$$

Let us still choose the computational domain $\Omega = (0, 1) \times (0, 1)$ with the uniform triangulation $T^h(\Omega)$. We consider a smooth problem with exact solution

$$u(x, y, t) = x^2(1-x)^2y(1-y)(1-2y)\cos(2\pi t). \tag{44}$$

Then the initial condition and f are obtained by (1) following the exact solution. For the finite element spaces, we choose the piecewise P_2 continuous finite element spaces as follows:

$$S^h(\Omega) = \{v \in C^0(\Omega) : v|_{\tau^h} \in P_{r,\tau^h}^2, \forall \tau^h \in T^h(\Omega)\}.$$

That means $r = 2$. So for Algorithm 3.1, while $\rho_{u,\Delta t,0}$ and $\rho_{u,h,0}$ approach 4.0 and 8.0, the convergence order will be 2.0 and 3.0, respectively.

In Table 1 we give the convergence order with respect to the time step Δt with the fix mesh size $h = 1/16$ and the varying time step length $\Delta t = 1/5, 1/10, 1/20$. And we fix the coarser grid triangulation $T^H(\Omega)$ with $H = 1/4$ to realize the partition of unity on Ω . These results display that the second convergence order with respect to the time step Δt . In Table 2, we present the results of convergence order with respect to h for Algorithm 3.1. In these experiments, we fix $\Delta t = 1/10$ and choose $h = 1/8, 1/16, 1/32$. And the numerical experiment results are consistent with the theoretical analysis.

6.3. Experiment 3: the parallel speedup

Notice that the accuracy of parareal method is determined by the accuracy of \mathcal{F} , which is used in serial. This conclusion also applies to the space-time parallel algorithm, Algorithm 3.1. So we define the parallel speedup, the ration of the serial to parallel cost, to verify the efficiency of parallel scheme. For the sake of content completeness, we provide the following serial second-order SDC algorithm (Algorithm 6.1).

Algorithm 6.1 (The spectral deferred correction method for the heat equation).

- Step 1. The prediction step of SDC: Compute $u_{1,h}^{n+1} \in S_0^h(\Omega)$, $n = 0, \dots, N - 1$, by using (12).
- Step 2. One iteration step of SDC based on (9)-(10): find $u_S^{n+1} \in S_0^h(\Omega)$, $n = 0, \dots, N - 1$, such that

$$\begin{cases} \left(\frac{u_S^{n+1} - u_S^n}{\Delta t}, v_h \right) + a(u_S^{n+1}, v_h) = a\left(\frac{u_{1,h}^{n+1} - u_{1,h}^n}{2}, v_h \right) + \left(\frac{f^{n+1} + f^n}{2}, v_h \right), \quad \forall v_h \in S_0^h(\Omega), \\ u_S^0 = P_h u^0 = 0. \end{cases}$$

Table 3

Comparisons of the serial and space-time parallel algorithms with $\Delta t = 1/64$.

Algorithm	$h = 1/8$		$h = 1/64$	
	Algorithm 6.1	Algorithm 3.1	Algorithm 6.1	Algorithm 3.1
$\ u^m - u_h^m\ _\Omega$	3.096e-4	3.027e-4	5.363e-6	5.527e-6
CPU(s)	1.691	0.53	100.5	34.78
Speedup	–	3.19	–	2.89

Table 4

The numerical errors at time $t^m = 1$ of Algorithm 6.2, with $\Delta t = 1/100$ and $h = 1/32$.

Iteration	$K = 2$	$K = 4$	$K = 6$	$K = 8$	$K = 10$
$\ u_{k,h}^m - u^m\ _\Omega$	2.024e-5	2.048e-5	2.077e-5	2.109e-5	2.149e-5

Now we are ready to analyze the computation of parallel speedup of our local and parallel space-time algorithm. We further discuss the allocation of processors for the spatial and temporal parallelism. We assume that each processor is identical and the communication time between the different processors is negligible. Recall that for the effectiveness of parareal method, \mathcal{G} must be computationally less expensive than \mathcal{F} . Let Y_G denote the computational time for one processor to compute one time step of the backward Euler method. For the correction procedure over $\Omega \times [t^n, t^{n+1}]$, the cost can be approximately equal to Y_G over each time step. Considering the computational time for one processor to compute one time step of the local residual equation based on \mathcal{F} , we denote the time over each subdomain Ω_j and the global domain Ω as Y_{F,Ω_j} and $Y_{F,\Omega}$, respectively. Notice that $N = T/\Delta t$ is the number of time subintervals and M is the number of subdomains. For the serial SDC algorithm (Algorithm 6.1), the total computational time is $NY_G + NY_{F,\Omega}$ with one processor. It is worth noting that even if we provide more processors, the total computational time of this serial scheme does not decrease. This is because one has to solve each step in sequence. Next, assume that there are NM' processors for our space-time parallel algorithm (Algorithm 3.1) with N time subintervals, so we distribute M' processors over each time step for the spatial parallelism. In addition, we utilize the idea of pipelined parareal [9] for the computational cost of time parallel. Hence, the space-time parallel speedup of Algorithm 3.1 is

$$S_{space,time} = \begin{cases} \frac{NY_G + NY_{F,\Omega}}{NY_G + Y_{F,\Omega_j} + Y_G}, & \text{if } M' > M, \\ \frac{NY_G + NY_{F,\Omega}}{NY_G + (\alpha + 1)Y_{F,\Omega_j} + Y_G}, & \text{if } \alpha M' < M \leq (\alpha + 1)M' \text{ and } \alpha \geq 0 \text{ is an integer.} \end{cases}$$

For simplicity, we pick the piecewise linear continuous finite element spaces

$$S^h(\Omega) = \{v \in C^0(\Omega) : v|_{\tau_\Omega^h} \in P_{\tau_\Omega^h}^1, \forall \tau_\Omega^h \in T^h(\Omega)\}.$$

We still consider the computational domain $\Omega = (0, 1) \times (0, 1)$ and the exact solution (44) for the heat equation (1). Let us fix the time step length $\Delta t = 1/64$. And we fix the grid triangulation $T^H(\Omega)$ with $H = 1/4$ to obtain the partition of unity on Ω . Assume that there are 950 processors, so there are 15 processors over each time step used for the spatial parallelism in our space-time parallel algorithm (Algorithm 3.1). Next, we denote u_h^m as the numerical solutions at time t^m . Table 3 shows the L^2 -error between the numerical solutions and true solution, CPU time and the parallel speedup results. So, with almost the same accuracy, our space-time parallel algorithm has the lower CPU time than the serial algorithm.

6.4. Experiment 4: the space-time parallel algorithm with more iterations

In fact, the parareal method is one kind of iterate methods, which proceeds iteratively alternating between the parallel computation of \mathcal{F} and the serial computation of \mathcal{G} . However there are only two iterations in our algorithms. Next, we take Algorithm 3.1 as an example to show the reasons why there are no more iterations in this parallel algorithm. First of all, Experiment 2 has verified that Algorithm 3.1 has second-order convergence in time. Next, we give the space-time parallel iterative algorithm, Algorithm 6.2. Here, we denote $K \geq 2$ as the number of iterations. Obviously, when $K = 2$, it is Algorithm 3.1.

Algorithm 6.2 (The space-time parallel iterative algorithm).

- Step 1. Let $k = 1$ and compute $u_{1,h}^{n+1} := \mathcal{G}(t^{n+1}, t^n, u_{1,h}^n) \in S_0^h(\Omega)$, $n = 0, \dots, N - 1$, by using (12) in serial.
- Step 2. Compute $u_F^{n+1} := \mathcal{F}(t^{n+1}, t^n, u_{k,h}^n) \in S_0^h(\Omega)$, $n = 0, \dots, N - 1$ in parallel by using the same methods in Step 2 of Algorithm 3.1.
- Step 3. Compute $u_G^{n+1} := \mathcal{G}(t^{n+1}, t^n, u_{k+1,h}^n) \in S_0^h(\Omega)$, $n = 0, \dots, N - 1$, by using (18) in serial. Then, we update the approximate solution $u_{k+1,h}^{n+1} = u_G^{n+1} + u_F^{n+1} - u_{k,h}^{n+1}$ with the initial value $u_{k+1,h}^0 = P_h u^0 = 0$.
- Step 4. Let $k = k + 1$. If $k = K$, then stop. Otherwise, go to Step 2.

Let us compute the errors between the exact solution and numerical solution of Algorithm 6.2 with different iterations. We still consider the same computational domain, triangulation and exact solution as Experiment 1. If we take $\Delta t = 1/100$ and $h = 1/32$, the numerical error at time $t^m = 1$ of the serial second-order SDC method (Algorithm 6.1) is 2.056e-5. We compute the numerical errors of Algorithm 6.2 and show these results in Table 4. We can find that, as the number of iterations increases, the errors also increase. That is, the accuracy is not improved with the increase of iterations. And the iterative algorithm with $K = 2$, Algorithm 3.1, can obtain almost the same accuracy as the serial algorithm (Algorithm 6.1). Therefore, two iterations are enough to get the results we want.

7. Conclusion

In this paper, we propose a local and parallel space-time scheme for the heat equation based on the parareal with spectral deferred correction and the expandable local and parallel finite element methods. We prove the stability and second-order accuracy in time of our space-time parallel algorithm. At last, the numerical experiments verify the effectiveness of our scheme. In the future work, in order to verify the practicality of this space-time parallel algorithm, we will apply this idea to more complex systems, such as the Navier-Stokes/Darcy system, the Cahn–Hilliard equations and so on. On the other hand, we will consider other parallel methods, such as the local and parallel two-grid method, to further improve the speedup and accuracy of parallel algorithms.

Acknowledgements

This work is supported by the National Natural Science Foundation of China (Nos. 11971378, 11571274 and 12101494), the Natural Science Foundation of Shaanxi Province (No. 2021JQ-426) and the Scientific Research Program funded by Education Department of Shaanxi Provincial Government (No. 21JK0935).

References

- [1] J.L. Lions, Y. Maday, G. Turinici, A “parareal” in time discretization of PDE’s, *C. R. Acad. Sci., Ser. I Math.* 332 (7) (2001) 661–668.
- [2] G.A. Staff, E.M. Rønquist, *Stability of the Parareal Algorithm*, Springer Berlin Heidelberg, 2005.
- [3] M.J. Gander, E. Hairer, *Nonlinear Convergence Analysis for the Parareal Algorithm*, Springer Berlin Heidelberg, 2008.
- [4] M.J. Gander, S. Vandewalle, On the superlinear and linear convergence of the parareal algorithm, in: *Domain Decomposition Methods in Science and Engineering XVI*, vol. 55, Springer Berlin Heidelberg, 2007, pp. 291–298.
- [5] G. Bal, On the convergence and the stability of the parareal algorithm to solve partial differential equations, in: *Domain Decomposition Methods in Science and Engineering*, Springer Berlin Heidelberg, 2005, pp. 425–432.
- [6] M.J. Gander, S. Vandewalle, Analysis of the parareal time-parallel time-integration method, *SIAM J. Sci. Comput.* 29 (2) (2007) 556–578.
- [7] E. Aubanel, Scheduling of tasks in the parareal algorithm, *Parallel Comput.* 37 (3) (2011) 172–182.
- [8] M.L. Minion, S.A. Williams, Parareal and spectral deferred corrections, *AIP Conf. Proc.* 1048 (1) (2008) 388–391.
- [9] M.L. Minion, A hybrid parareal spectral deferred corrections method, *Commun. Appl. Math. Comput. Sci.* 5 (5) (2011) 265–301.
- [10] C. Farhat, M. Chandesris, Time-decomposed parallel time-integrators: theory and feasibility studies for fluid, structure, and fluid-structure applications, *Int. J. Numer. Methods Eng.* 58 (2003) 1397–1434.
- [11] M. Bolten, D. Moser, R. Speck, A multigrid perspective on the parallel full approximation scheme in space and time, *Numer. Linear Algebra Appl.* 24 (2017).
- [12] S. Bu, J.Y. Lee, An enhanced parareal algorithm based on the deferred correction methods for a stiff system, *J. Comput. Appl. Math.* 255 (285) (2014) 297–305.
- [13] Y. Maday, J. Salomon, G. Turinici, Monotonic parareal control for quantum systems, *SIAM J. Numer. Anal.* 45 (6) (2007) 2468–2482.
- [14] X. Dai, Y. Maday, Stable parareal in time method for first- and second-order hyperbolic systems, *SIAM J. Sci. Comput.* 35 (1) (2013) A52–A78.
- [15] P.F. Fischer, F. Hecht, Y. Maday, *A Parareal in Time Semi-implicit Approximation of the Navier-Stokes Equations*, Springer Berlin Heidelberg, 2005.
- [16] D. Xue, Y. Hou, W. Liu, Analysis of the parareal method with spectral deferred correction method for the Stokes/Darcy equations, *Appl. Math. Comput.* 387 (2020) 124625.
- [17] C. Farhat, J. Cortial, C. Dastillung, H. Bavestrello, Time-parallel implicit integrators for the near-real-time prediction of linear structural dynamic responses, *Int. J. Numer. Methods Eng.* 67 (5) (2010) 697–724.
- [18] T.P. Mathew, M. Sarkis, C.E. Schaerer, Analysis of block parareal preconditioners for parabolic optimal control problems, *SIAM J. Sci. Comput.* 32 (3) (2010) 1180–1200.
- [19] Y. Hou, G. Du, An expandable local and parallel two-grid finite element scheme, *Comput. Math. Appl.* 71 (12) (2016) 2541–2556.
- [20] J. Xu, A. Zhou, Local and parallel finite element algorithms based on two-grid discretizations, *Math. Comput.* 69 (231) (2000) 881–909.
- [21] J. Xu, A. Zhou, Local and parallel finite element algorithms based on two-grid discretizations for nonlinear problems, *Adv. Comput. Math.* 14 (4) (2001) 293–327.
- [22] Y. He, J. Xu, A. Zhou, J. Li, Local and parallel finite element algorithms for the Stokes problem, *Numer. Math.* 109 (3) (2008) 415–434.
- [23] G. Du, L. Zuo, Local and parallel finite element post-processing scheme for the Stokes problem, *Comput. Math. Appl.* 73 (1) (2017) 129–140.
- [24] Y. He, J. Xu, A. Zhou, Local and parallel finite element algorithms for the Navier-Stokes problem, *J. Comput. Math.* (2006) 227–238.
- [25] J. Xu, A. Zhou, Local and parallel finite element algorithms for eigenvalue problems, *Acta Math. Appl. Sin.* 18 (2) (2002) 185–200.
- [26] Q. Liu, Y. Hou, Local and parallel finite element algorithms for time-dependent convection-diffusion equations, *Appl. Math. Mech.* 30 (6) (2009) 787–794.
- [27] A. Dutt, L. Greengard, V. Rokhlin, Spectral deferred correction methods for ordinary differential equations, *BIT Numer. Math.* 40 (2) (2000) 241–266.
- [28] M.L. Minion, Semi-implicit projection methods for incompressible flow based on spectral deferred corrections, *Appl. Numer. Math.* 48 (3) (2004) 369–387.
- [29] M.L. Minion, Semi-implicit spectral deferred correction methods for ordinary differential equations, *Commun. Math. Sci.* 1 (3) (2002) 2127–2157.
- [30] C. Bernardi, A.Y. Orfi, A priori error analysis of the fully discretized time-dependent coupled Darcy and Stokes equations, *SeMA J.* 38 (3) (2004) 1–23.
- [31] M. Mu, X. Zhu, Decoupled schemes for a non-stationary mixed Stokes-Darcy model, *Math. Comput.* 79 (270) (2010) 707–731.
- [32] D. Xue, Y. Hou, Numerical analysis of a second order algorithm for a non-stationary Navier–Stokes/Darcy model, *J. Comput. Appl. Math.* 369 (2020).
- [33] F. Collino, P. Joly, F. Millot, Fictitious domain method for unsteady problems, *J. Comput. Phys.* 138 (2) (1997) 907–938.
- [34] V. Girault, R. Glowinski, H. López, J.-P. Vila, A boundary multiplier/fictitious domain method for the steady incompressible Navier-Stokes equations, *Numer. Math.* 88 (1) (2001) 75–103.
- [35] F. Hecht, New development in freefem++, *J. Numer. Math.* 20 (3–4) (2012) 251–266.